

## ON THE POMERON STRUCTURE FUNCTION IN QCD

J. BARTELS

*II. Institut für Theoretische Physik, Universität Hamburg, D-2000 Hamburg, FRG*

and

G. INGELMAN

*Department of Radiation Sciences, Uppsala University, Box 535, S-751 21 Uppsala, Sweden*

Received 9 November 1989

The concept of a pomeron structure function, introduced in connection with "hard diffractive scattering", is here discussed in terms of gluon ladders and fan diagrams in perturbative QCD. We find that the gluon distribution of the pomeron is in many cases dominated by non-perturbative effects, which support earlier work based on Regge theory. There are cases, however, where perturbative QCD effects dominate and the Regge-based treatment is incorrect. In all cases, perturbative QCD can be used to gain understanding of the pomeron and give predictions to be tested at  $p\bar{p}$  colliders and at HERA.

Strong interaction processes at large energies, but with small momentum transfers are not yet explained within QCD due to our lack of understanding the confinement mechanism. In particular, the nature of the pomeron is not understood in spite of a wealth of experimental data on elastic and diffractive scattering [1]. It has been suggested [2] that the pomeron may be a system of gluons [3] and as an attempt to obtain experimental information about such a possible parton content it was suggested [4] to search for hard scattering phenomena in high mass diffractive scattering at collider energies. In the model of ref. [4], the exchanged pomeron is viewed as a "quasi"-particle, emitted from one beam proton and colliding with an opposite beam (anti)proton, and a pomeron structure function was introduced to measure its parton content in analogy to a real hadron. Recent collider data from UA8 [5] give strong evidence for transverse jets in diffractively excited high mass systems, which can only be understood as hard scattering of partons. The data are, furthermore, in reasonable agreement with the model in ref. [4] using a rather soft gluon momentum distribution in the pomeron. This model has also been applied to other processes such as heavy flavour production [6,7] and

deep inelastic scattering [8,9]. It has furthermore been discussed in ref. [7] how the description of hadronic inclusive cross-sections in terms of Regge theory, in the triple Regge limit, might be used as a theoretical motivation for this phenomenological approach. In these studies, the pomeron structure function has always been seen as a new and a priori unknown quantity. In an alternative approach [10], the pomeron is argued to couple to single quarks rather like a  $C = +1$  photon and hence its structure be dominated by a quark-antiquark component in analogy with the photon structure function.

In this paper we want to examine the concept of a pomeron structure function in terms of perturbative QCD. We therefore consider to probe this function in deep inelastic scattering in order to have a cleaner situation in analogy to the theoretical treatment and experimental measurements of the proton structure function. Thus, we envisage a pomeron, which is "emitted" from a proton, to be probed by a virtual photon in electron scattering [4]. In particular at HERA, this could provide high resolution measurements of the parton structure in the pomeron [9]. The experimental signature would be quite clear: a quasi-elastically scattered proton (at a very small an-

gle) well separated (e.g. in rapidity) from the remaining hadronic system that experiences the deep inelastic scattering, as illustrated in fig. 1a.

In previous investigations it has been assumed that the pomeron stays "soft", i.e. does not have any large momentum transfers between its constituent partons, until it combines with the other incoming particle and produces the final state with mass  $M_X$ . In the normal analysis of deep-inelastic scattering the momentum square  $q^2 \approx q_1^2$  of the quarks and gluons may, however, vary from some low scale  $Q_0^2$  up to  $Q^2$  of the virtual photon, as described by the well-known Gribov-Lipatov-Altarelli-Parisi equations in QCD [11]. When applying this evolution picture to the process as viewed in the Regge theory framework, where the squared scattering amplitude is shown in fig. 1b, it is a priori not known how much of this evolution that takes place already "inside the pomeron", below the "triple pomeron vertex" and how much is left for the upper part of the diagram. Most generally one expects an integration over all possibilities, i.e. an integral over the scale  $q^2$  at the triple vertex. Since the two-pomeron exchange in the lower part of fig. 1b corresponds to higher twist with a factor  $1/q^2$ , we expect that the small- $q^2$  region will be enhanced compared to larger values of  $q^2$ . The details of the distribution in  $q^2$  will, however, depend on a non-trivial balance between the different parts in fig. 1b.

To analyse these aspects of the pomeron structure function in perturbative QCD we suggest that the proper framework is that of QCD ladders and fan

diagrams as studied and reviewed by Gribov, Levin and Ryskin [12]. The QCD analog of the Regge diagram in fig. 1b is shown in fig. 1c, where each pomeron corresponds to a QCD ladder (with the energy discontinuity through the upper ladder, but not through the lower ones). The large- $q^2$  region should then be calculable in perturbative QCD. In the following we therefore want to formulate a QCD based treatment of the pomeron structure function and perform numerical evaluations in order to investigate how much information can be obtained from perturbative QCD. The low- $q^2$  part of the pomeron is still non-perturbative, but it may not be too far away from a naive extrapolation of the perturbative region. Thus, we want to examine to what extent one can obtain a smooth transition from perturbative QCD to the earlier approaches based on Regge theory; this could give additional justification to the latter.

Our starting point is the perturbative QCD formula for the fan diagram in fig. 1c, as given by eq. (6.12) in ref. [12]:

$$\frac{d^2\sigma}{dt dM^2} \sim \int_{Q_{had}^2}^{Q^2} dq^2 \tilde{\phi}(x/x_M, Q^2, q^2) \alpha_s^2(q^2) g \times \phi^2(x_M, q^2; t) . \tag{1}$$

Here  $x = Q^2/2pq$  is the usual Bjorken variable, and  $x_M = (M_X^2 + Q^2)/(s + Q^2)$  is the fraction of the proton momentum carried by the pomeron. As before,

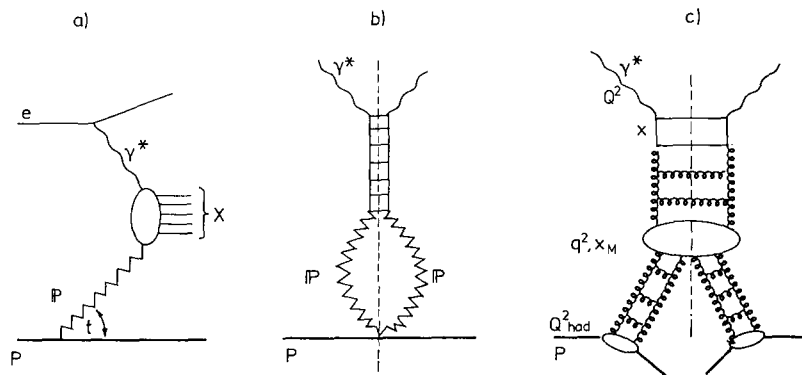


Fig. 1. The pomeron structure function measured in deep inelastic scattering. (a) The general diagram with produced hadronic system X. (b) The squared scattering amplitude in the Regge framework. (c) The squared scattering amplitude in terms of perturbative QCD ladders.

$q^2$  denotes the (internal) momentum scale at the triple pomeron vertex where the coupling  $\alpha_s^2(q^2)g$  enters. The function  $\tilde{\phi}(x/x_M, Q^2, q^2)$  is for the upper QCD ladder in fig. 1c. It represents the probability to find a parton of virtuality  $Q^2$  and momentum fraction  $x$ , with respect to the proton, at the top of the ladder when a parton of virtuality  $q^2$  and momentum fraction  $x_M$  enters at the bottom of the ladder. The parton at the photon vertex has the fraction  $z=x/x_M$  of the exchanged pomeron momentum. Similarly, the two lower ladders each contribute a factor  $\phi$  which is related to the normal parton density distribution by a derivative, with respect to the upper momentum scale, to give a definite parton virtuality  $q^2$  at the triple vertex. The integral over  $q^2$  in eq. (1) is one of the crucial differences between our new approach for the pomeron structure function and the earlier ones [4,7].

Eq. (1) is, in fact, very closely related to the expression for the first fan diagram [12], which has been proposed as the first correction in the small- $x$  limit to the standard QCD evolution of the proton structure function. The reason for this lies in the validity [12] of the Abramovsky–Gribov–Kanchelli (AGK) cutting rules, which relate the different energy discontinuities of a diagram like that of fig. 1b to each other (diffractive cut, multiperipheral cut, double multiperipheral cut). There is, however, also an important difference between eq. (1) and the formula for the first fan diagram: this is the lower limit of the  $q^2$  integration. In eq. (1) the integral has to begin at a low momentum scale  $Q_{\text{had}}^2 \approx 1 \text{ GeV}^2$  corresponding to a typical hadron mass, i.e. the proton at the bottom of fig. 1c. In the fan diagram for the proton structure function, on the other hand, the lower limit  $Q_0^2$  should be a few  $\text{GeV}^2$  where a trustworthy QCD evolution starts. The region between  $Q_{\text{had}}^2$  and  $Q_0^2$ , with important non-perturbative effects, is then absorbed in the input distributions at  $Q_0^2$  to the normal evolution procedure. Another difference concerns the  $t$  dependence in eq. (1): the fan diagram contribution to the proton structure function includes an integration over  $t$  (although  $t$  is restricted to rather small values), whereas the pomeron structure function is defined for fixed  $t$  values.

In the following we want to study certain qualitative aspects of eq. (1), in particular the significance of the  $q^2$  integration. For a first estimate, we find it

convenient to simplify this formula in several ways. First, we shall consider only gluon contributions to  $\tilde{\phi}$ ,  $\phi$ ,  $\alpha_s^2 g$ . This is justified as long as both  $x_M$  and  $z=x/x_M$  are small. Secondly, as the simplest model for the triple pomeron vertex we use the planar loop (fig. 2.7 in ref. [12]), expecting that it will give the correct order of magnitude and qualitative dependence on  $q^2$ . These simplifications allow us to use Kwiecinski's expression [13] for the fan diagram which has been tested numerically. For the momentum weighted pomeron structure function we therefore obtain

$$zP(z=x/x_M; x_M, Q^2) = \frac{1}{4R^2} \int_{Q_{\text{had}}^2}^{Q^2} dq^2 D(Y-Y_M, Q^2, q^2) \left( \frac{3\alpha_s(q^2)}{q^2} \right)^2 \times G^2(Y_M, q^2, Q_0^2). \quad (2)$$

Here,  $Y=\ln(1/x)$ ,  $Y_M=\ln(1/x_M)$ , and the functions  $D$  and  $G$ , which are the analogues of  $\tilde{\phi}$  and  $\phi$  in eq. (1), are given explicitly in ref. [13] (by lengthy expressions not reproduced here). Again, the lower limit of the integration has to be lower than  $Q_0^2$ , taken as  $5 \text{ GeV}^2$  in ref. [13], and the extension needed will be discussed below. Eq. (2) also includes an integral over small  $t$  values and thus represents a “ $t$ -integrated” pomeron structure function. We will use eq. (2) also in the region  $z=x/x_M \rightarrow 1$ , although quark contributions cannot really be neglected there. In this region the expression for the structure function  $D$  in eq. (2) is not applicable and we therefore use the approximate form

$$D(Y-Y_M, Q^2, q^2) = e^{A\xi} (1-x/x_M)^{4N_c\xi}, \quad (3)$$

which we derived from a set of QCD ladder diagrams satisfying the Altarelli–Parisi equations in  $Q^2$ , but with the proper initial condition  $D=1$  at  $Q^2=q^2$ . Here, the constant  $A = -4N_c\gamma_E + \frac{11}{3}N_c - \frac{2}{3}n_f$  is given in terms of the number of colours and flavours,  $N_c=3$  and  $n_f=4$ , and the Euler constant,  $\gamma_E$ . The  $Q^2$  dependence is through  $\xi = \ln[\ln(Q^2/\Lambda^2)] - \ln[\ln(q^2/\Lambda^2)]$ . A similar power behavior in  $1-z$  also holds in the presence of quarks, but with a different ( $\xi$ -dependent) exponent.

For our numerical analysis we first investigate which values of  $q^2$  give the most important contributions to the integral in eq. (2). This is shown in fig. 2, where the integrand of (2) is plotted versus  $q^2$

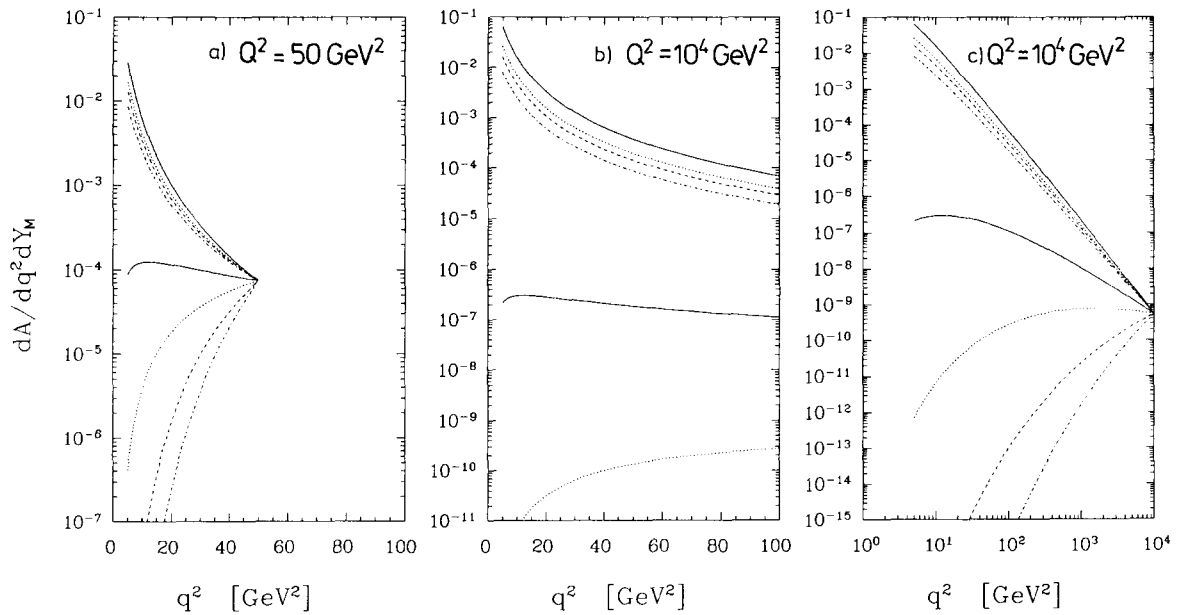


Fig. 2. Integrand of eq. (2) as a function of the momentum scale  $q^2$  at the triple pomeron vertex, for a momentum transfer scale of (a)  $Q^2 = 50 \text{ GeV}^2$  and (b), (c)  $Q^2 = 10^4 \text{ GeV}^2$  at the upper vertex (e.g. given by the virtual photon). In all cases  $x_M = 0.05$  and the curves are, starting from the top, for  $z = x/x_M = 0.01, 0.05, 0.1, 0.25$  using  $D$  from ref. [13] and  $z = 0.5, 0.75, 0.9, 0.95$  using  $D$  in eq. (3).

for some illustrative cases. We have chosen  $x_M = 0.05$  since this corresponds to a Feynman- $x$  of the quasi-elastically scattered proton of  $x_F = 1 - x_M = 0.95$ , which is central in the interval  $0.9-1$  usually considered for diffractive processes. In particular, it matches the central value for the UA8 data [5]. To illustrate the  $Q^2$  dependence we use both a lower value,  $50 \text{ GeV}^2$  which is in the region of the UA8 data, and a large one,  $10^4 \text{ GeV}^2$ . For the momentum fraction  $z = x/x_M$  of the struck parton in the pomeron we take the values  $0.01, 0.05, 0.1, 0.25$  and  $0.5, 0.75, 0.9, 0.95$  to study the behaviour at both small and large  $z$ , where in the first case the  $D$  function can be taken from Kwiecinski [13] and in the second case we use eq. (3). For small  $z$ , fig. 2 shows a strong peaking towards low- $q^2$  values. This is the result of the  $1/q^2$  factors in eq. (2) which relate to the higher twist nature of these QCD diagrams. Consequently, one can in this case obtain a reasonable approximation to the  $q^2$  integral in (2), by simply disregarding all values higher than a few  $\text{GeV}^2$ . This justifies the treatment of refs. [4-9], which did not consider any integration over  $q^2$ . Comparing figs. 2a and 2b, one observes that the

peaking at low  $q^2$  is slightly less pronounced at larger  $Q^2$ . In contrast, the peaking depends very strongly on  $z$ , such that for  $z \geq 0.5$  the peaking at low  $q^2$  disappears and is, for  $z \rightarrow 1$ , replaced by a peaking at  $q^2 = Q^2$ . This is easily understood from the power of  $1-z$  in eq. (3) which increases with  $\xi$ ; in order to have the maximal contribution for  $z$  close to 1, the power should be as small as possible, which happens for  $q^2$  close to  $Q^2$ . This dominance of large  $q^2$  values should remain valid also when quarks are included. It follows from this observation that for  $z \geq 0.5$  the integration over  $q^2$  is essential, and the Regge-based treatment of refs. [4-9] is not applicable, although both  $M^2$  and  $s/M^2$  are large enough to make the triple Regge formalism valid in principle.

In order to calculate the pomeron structure function from eq. (2) we have to examine the low- $q^2$  region more closely. Since this equation has been derived from perturbative QCD, we can, initially, not go below  $Q_0^2$  where the validity of perturbation theory starts. For this reason our curves in fig. 2 start at  $q^2 = Q_0^2 = 5 \text{ GeV}^2$  chosen in ref. [13]. We have, however, no justification to exclude the region  $Q_{\text{had}}^2 \leq$

$q^2 \leq Q_0^2$ . On the contrary, our curves in fig. 2 indicate that, for small  $z$ , this region will even give the essential contribution! Rather than taking the attitude that eq. (2) is useless for this case, one may simply extrapolate the perturbative integrand down to values below  $5 \text{ GeV}^2$  and examine how much the resulting pomeron structure function deviates from the ones assumed in ref. [4] and compared with data in ref. [5]. Such a procedure has some justification, since the lower part of fig. 1b satisfies a (modified) evolution equation [14] which could be used to perform an evolution starting at a smaller value of  $Q_0^2$  than  $5 \text{ GeV}^2$ . When applying this idea one encounters the somewhat unpleasant feature that the integrand of eq. (2) reaches a maximum at  $q^2 \approx 2.5 \text{ GeV}^2$  and falls rapidly below. Although this is an artifact of the Bessel functions used in Kwiecinski's expression for  $G$  and the choice of parameters, the flattening off is quite reasonable. In fact, one does not expect the integrand of eq. (2) to rise ad infinitum for  $q^2 \rightarrow 0$ , but to reach

a maximum at a typical hadronic scale of, say,  $1 \text{ GeV}^2$ . With the choice of parameter values ( $Q_0^2 = 5 \text{ GeV}^2$ ,  $A = 0.29 \text{ GeV}$ ) used in ref. [13] the maximum is, however, reached at a too high value of  $q^2$ . Since there is a freedom in these values (related to the uncertainties in parton distributions of the proton) we may change them slightly for the purpose of making the extrapolation to  $Q_{\text{had}}^2$ . For example, taking  $Q_0^2 = 2 \text{ GeV}^2$  and  $A = 0.18 \text{ GeV}$ , the  $q^2$  dependence of  $G$  is practically unchanged for  $q^2 > 10 \text{ GeV}^2$  (the deviations from the curves for  $xg(x, Q^2)$  in ref. [13] are limited to 10%), whereas in the low- $q^2$  region the maximum moves down to some value below  $1 \text{ GeV}^2$ . In fig. 3 we show the integrand in eq. (2) over the full range  $Q_{\text{had}}^2 = 1 \text{ GeV}^2 \leq q^2 \leq Q^2$  using this extrapolation method.

We can now calculate the full integral over  $q^2$  and obtain the pomeron structure function shown in fig. 4, where the solid and dashed curves correspond to the small- $z$  and large- $z$  approximations for the func-

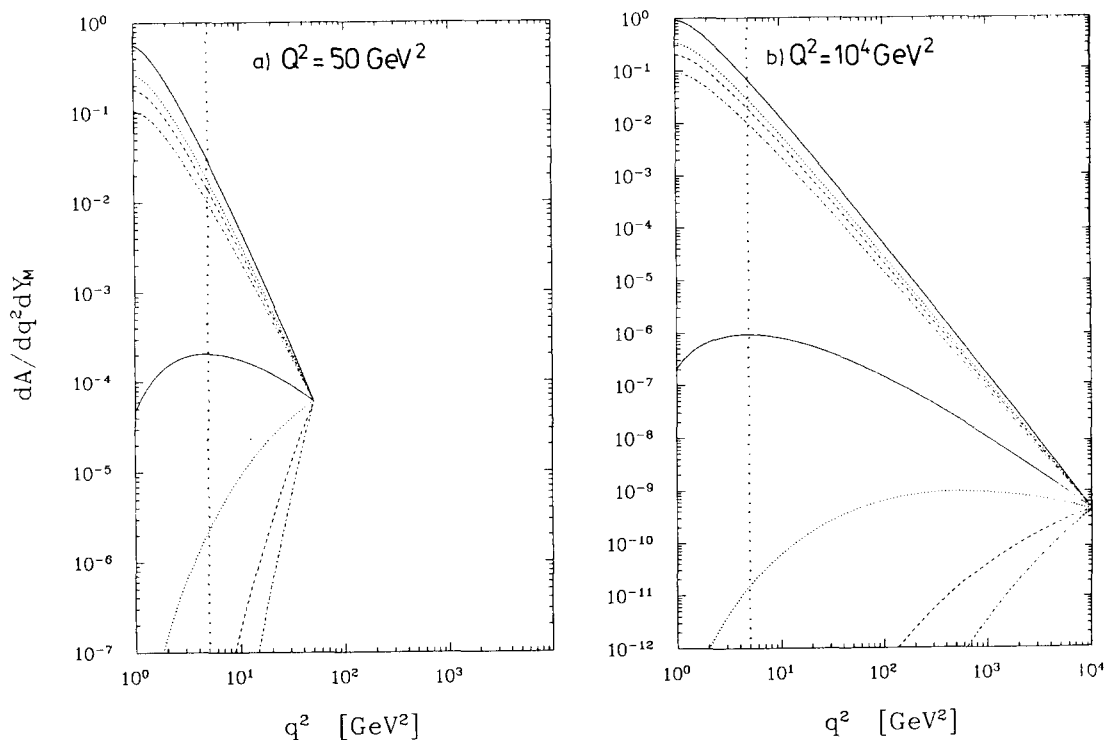


Fig. 3. Modified integrand of eq. (2) as discussed in the text, with extrapolation in  $q^2$  below  $Q_0^2 = 5 \text{ GeV}^2$  (marked by the vertical dotted line) to  $Q_{\text{had}}^2 = 1 \text{ GeV}^2$ .

tion  $D$ , respectively. The former becomes unreliable for large  $z$  and should not be taken seriously for  $z \gtrsim 0.1$ . The final result should therefore be given by a smooth transition from the solid curve at small  $z$  to the dashed curve at large  $z$ , although this is not explicitly shown in fig. 4. This pomeron structure function from perturbative QCD can now be compared to the ones considered in refs. [4–9]. In particular, we show by dotted curves in fig. 4 the forms  $N(1-z)^5$  and  $Nz(1-z)$  used in ref. [4,5]. The normalisation constant,  $N$ , does here also include the integral over the  $t$  dependence of single diffraction as given in ref. [4]. This is needed in the comparison with eq. (2) which actually contains the integral over the momentum transfer,  $t$ , at the lower vertex in fig. 1a. The first, soft gluon distribution is supported by the UA8 data [5], and it is pleasing to see that our “calculated” pomeron structure function has a similar shape. The fact that our function is lower in normalization should not be taken too seriously at this stage. The exact form of the exponential  $t$  dependence at low  $t$  is not known and gives, therefore, an uncertainty in the integral just mentioned. In addition, our result for the integral, i.e.  $zP(z)$ , has some uncertainty related to the exact

choice of the lower integration limit  $Q_{\text{had}}^2$  which is, furthermore, in the region of our rather crude extrapolation. More fundamentally, one should also add a contribution from quarks in the QCD ladders, which were neglected in our treatment. At this stage we have to be content with the observation that there seems to be no dramatic change between the perturbative and the low- $q^2$  region. In further developments of this QCD treatment of the pomeron structure function, the quark contributions should be included and the above approximations be replaced with a more complete leading log evolution. Perturbative QCD might then be used to calculate the pomeron structure function more reliably.

To conclude, we have introduced the idea that the pomeron structure function can be related to the gluon ladders and fan diagrams in perturbative QCD and have thereby given a link between Regge and QCD diagrams for pomeron exchange. Our results have illustrated that in certain kinematic regions the pomeron is mainly the same, “soft” pomeron which describes the Regge limit of, e.g., elastic scattering in purely hadronic reactions. This is the case for  $z = x/x_M \lesssim 0.5$ , where the integral in eq. (2) is strongly

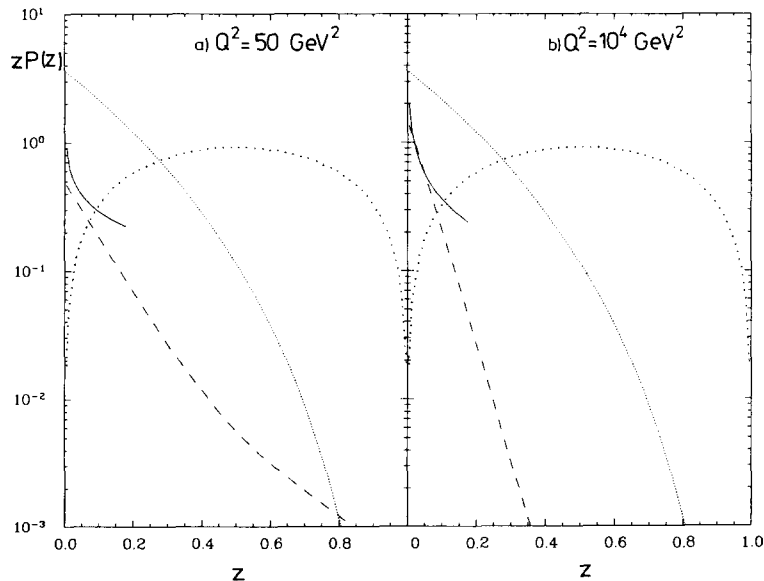


Fig. 4. The momentum-weighted pomeron structure function,  $zP(z)$ , obtained from eq. (2) for (a)  $Q^2=50 \text{ GeV}^2$  and (b)  $Q^2=10^4 \text{ GeV}^2$ . The solid and dashed curves are based on the small- $z$  and large- $z$  approximations discussed in the text. The dotted curves are the forms  $zP(z)=N(1-z)^5$  and  $Nz(1-z)$  used in refs. [4,5] (here,  $N=6 \times 3.4/5.6$  as motivated in the text).

dominated by very small  $q^2$  values. However, there are also cases ( $z \gtrsim 0.5$ ) where larger values of  $q^2$  are equally, or even more important, in which case the pomeron is not a "soft" object. In this case, the pomeron structure function can be completely calculated in perturbative QCD. Although this corresponds to lower cross sections, experimental tests of using events with  $z$  close to 1 might be possible. In ep collisions at HERA this would imply final states where  $x$  is not much less than  $x_M \ll 1$ , i.e. the momentum fraction of the pomeron should be small and close to Bjorken- $x$ . For such events the internal momentum scale at the triple pomeron vertex, which is approximately equal to the transverse momentum square of the partons, should be large compared to the hadronic mass scale. The pomeron spectator jet, i.e. the analog of a hadron beam remnant jet, could then be wider and shifted in angle from the pomeron momentum direction. Similar effects will occur in hard diffractive scattering at  $p\bar{p}$  colliders. Here, the large- $z$  region should be probed with very high transverse momentum jets or through production of massive states such as the  $W$  and  $Z^0$  bosons.

One of us (GI) is grateful for the hospitality of DESY where part of this work was made.

*Note added.* After completing this paper we received a paper by L. Frankfurt and M. Strikman investigating diffraction dissociation at large momentum transfer  $t$  which should allow the use of perturbative QCD for the pomeron. There is no di-

rect overlap between their paper and ours, but we consider their results as another evidence for the importance of diffractive dissociation as a new testing ground of QCD.

## References

- [1] For reviews see e.g. U. Amaldi, M. Jacob and G. Matthiae, *Annu. Rev. Nucl. Sci.* 26 (1976) 385; K. Goulianos, *Phys. Rep.* 101 (1983) 169.
- [2] S. Nussinov, *Phys. Rev. Lett.* 34 (1975) 1286; *Phys. Rev. D* 14 (1976) 246; F. Low, *Phys. Rev. D* 12 (1976) 163.
- [3] For a review see e.g. J. Bartels, preprint DESY 89-079, in: *Proc. 3rd Blois Workshop Intern. Conf. on Elastic and diffractive scattering* (Northwestern University, IL, May 1989).
- [4] G. Ingelman and P. Schlein, *Phys. Lett. B* 152 (1985) 256.
- [5] UA8 Collab., R. Bonino et al., *Phys. Lett. B* 211 (1988) 239.
- [6] H. Fritzsche and K.H. Streng, *Phys. Lett. B* 164 (1985) 391.
- [7] E.L. Berger, J.C. Collins, D.E. Soper and G. Sterman, *Nucl. Phys. B* 286 (1987) 704.
- [8] N. Atreaga-Romero, P. Kessler and J. Silva, *Mod. Phys. Lett. A* 1 (1986) 211.
- [9] K.H. Streng, in: *Proc. HERA Workshop* (Hamburg, 1987), ed. R.D. Peccei (DESY, Hamburg, 1988) Vol. 1, p. 365.
- [10] A. Donnachie and P.V. Landshoff, *Phys. Lett. B* 191 (1987) 309; *Nucl. Phys. B* 303 (1988) 634.
- [11] V.N. Gribov and L.N. Pipatov, *Yad. Fiz.* 15 (1972) 781, 1218 [*Sov. J. Nucl. Phys.* 15 (1972) 438, 675]; G. Altarelli and G. Parisi, *Nucl. Phys. B* 126 (1977) 298.
- [12] L.V. Gribov, E.M. Levin and M.G. Ryskin, *Phys. Rep.* 100 (1983) 1.
- [13] J. Kwiecinski, *Z. Phys. C* 29 (1985) 147.
- [14] A.H. Mueller and J. Qiu, *Nucl. Phys. B* 268 (1986) 427.